

DEVELOPMENT OF FLAME-RETARDED PLA COMPOSITIONS BY 3D PRINTING OF CORE-SKIN STRUCTURES

A. Regazzi¹, M.F. Pucci^{1*}, L. Dumazert¹, S. Buonomo¹, B. Gallard¹, R. Ravel¹, J.-M. Lopez Cuesta¹

¹C2MA, IMT Mines Ales, Univ Montpellier, Ales, France

*Email: monica.pucci@mines-ales.fr

Keywords: additive manufacturing, 3D printing, bio-based polymers, fire behaviour

Abstract

This work focused on the development of flame-retarded PLA compositions for additive manufacturing. Fused Filament Fabrication (FFF) was chosen as a technique to produce plate samples. Injected samples were also manufactured for comparison purpose. The nature of the flame retardants (FR), their contents and their distribution in the samples were varied. The microstructure was assessed in order to be related to fire performance of flame-retarded PLA structures. Fire behaviour was investigated *via* cone calorimeter tests. The results showed a significant decrease of the time to ignition (TTI) of 3D printed compared to injected samples, due to their higher porosity. However, for a given total FR content, concentrating FR close to the radiated surface proved to be a promising solution in order to optimise fire performance while preserving the mechanical properties of neat PLA.

1. Introduction

Poly lactide (PLA) is becoming one of the main biobased polymers used in 3D printing technology based on fused filament fabrication (FFF), analogous to fused deposition modeling (FDM®) [1]. As many polyesters, its use in many applications such as electronics, transportation and building requires its fire behaviour to be improved [6-8]. Intumescent systems based on ammonium polyphosphate (APP) and melamine (MEL) have proved to be effective to increase significantly the fire performance of PLA. Moreover, synergistic effects on fire properties can be achieved by adding nanofillers, such as organoclays of montmorillonite and sepiolite [2, 3, 9-13]. Nevertheless, high percentages of flame retardants (FR) tend to be detrimental to the ultimate mechanical properties [3]. To overcome these drawbacks, 3D printing technology allows core-skin structures to be produced in which flame retardant systems could be located only at the surface of the material exposed to the flame or radiant heat. These dual structures can be performed using dual extruder printers, enabling the sequential deposition of the core and the skin part. This way, it is possible to control the skin thickness in order to evaluate its influence on fire performance [4].

The aim of this study was to evaluate the performance of different formulations of flame-retarded PLA based on APP, MEL and organoclays by changing their overall content and their distribution regarding the exposed surface. For each formulation, injected and 3D printed samples were manufactured. Microstructure characterization and fire properties of 3D printed samples were investigated for these compositions and distributions in comparison with injected samples.

2. Materials and methods

2.1. Materials

Poly lactic acid (PLA) Ingeo™ Biopolymer 7000D from NatureWorks was used. In order to optimize its fire behaviour, the following FR were incorporated:

- Ammonium polyphosphate (APP): Exolit® AP 423 from Clariant;
- Melamine cyanurate (MC): Melapur® MC 15 from BASF;
- Montmorillonite organoclays (C30B): Cloisite® 30B from BYK;
- Sepiolite organoclays (PS9): Pangel S9 from Tolsa.

Five different compounds (F1, F2, F3, F4, F5) were processed, varying the amounts of the different FR in PLA in order to investigate their heat absorption, intumescence, and their possible synergies. Five analogous compositions (F1', F2', F3', F4', F5') with lower amounts of FR were also considered. Table 1 gives the contents of FR in PLA for all formulations.

Table 1. Studied formulations of flame-retarded PLA with respect to the FR contents [wt%]

Material	PLA	F1	F2	F3	F4	F5	F1'	F2'	F3'	F4'	F5'
PLA	100	85	82	82	97	97	96.25	95.5	95.5	99.25	99.25
APP	0	12	12	12	0	0	3	3	3	0	0
MC	0	3	3	3	0	0	0.75	0.75	0.75	0	0
C30B	0	0	3	0	3	0	0	0.75	0	0.75	0
PS9	0	0	0	3	0	3	0	0	0.75	0	0.75

2.2. Processing

2.2.1. Compounds

For every formulation FR were incorporated into PLA by dual extrusion with a BC21 extruder (900 mm) from Clextral.

2.2.2. Injection moulding

A fraction of each compound was used to produce 100×100×4mm³ plates (INJ) by injection moulding with a KM 50-180 CX unit from Krauss Maffei.

2.2.3. Additive manufacturing

The rest of each compound was used to produce calibrated filaments of 2.85 mm with a H2528 single extruder from Yvroud. The filament of each formulation was used in an A4v3 FFF machine from 3ntr so as to produce similar plates (3DP) of 100×100×4mm³. Nozzles of 0.4 mm in diameter were used to build 0.20 mm thick layers. The printing sequence was set as to deposit 2 contours for the outer shell of each layer and to alternate +45° and -45° infill patterns between every layer.

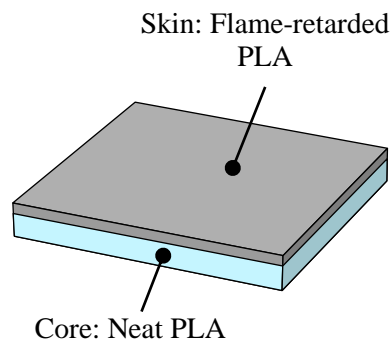


Figure 1. Skin/core structure of 3D printed samples (100×100×4mm³)

Since the FFF allows fabricating multi-material parts, skin-core structures were produced (cf. Figure 1) in order to evaluate the effect of limiting (or concentrating, depending on the FR content) the volume of

flame-retarded PLA close to the radiated surface during cone calorimeter tests (cf. 2.3.2). 3D printed samples are hereafter noted 3DP X mm where X stands for the thickness of flame-retarded PLA.

Depending on the formulation and the thickness of flame-retarded PLA, the total FR content may vary in the whole sample (cf. Table 2).

Table 2. Total FR content [wt%] for each sample depending on its manufacturing process and its thickness of flame-retarded PLA

Processing	PLA	F1	F2	F3	F4	F5	F1'	F2'	F3'	F4'	F5'
INJ	0	15.0	18.0	18.0	3.00	3.00	3.75	4.50	4.50	0.75	0.75
3DP 4 mm	0	15.0	18.0	18.0	3.00	3.00	3.75	4.50	4.50	0.75	0.75
3DP 1 mm	-	3.75	4.50	4.50	0.75	0.75	-	-	-	-	-

2.3. Characterization

2.3.1. Microstructure

Weight and dimensions of all samples were measured. Based on these values, the apparent density ρ_{app} [g/cm³] was determined. Besides, absolute density ρ_{abs} [g/cm³] was assessed with an Accupyc 1330 pycnometer from Micromeritics. Finally, porosity Φ [%] was calculated according to Equation (Eq. 1).

$$\Phi = 100 \left(1 - \frac{\rho_{app}}{\rho_{abs}} \right) \quad (Eq. 1)$$

Microstructures were observed after carbon coating by means of a Quanta 200 FEG scanning electron microscope (SEM) from FEI Company, before and after cone calorimeter tests (to observe the char residue structure).

2.3.2. Fire behaviour

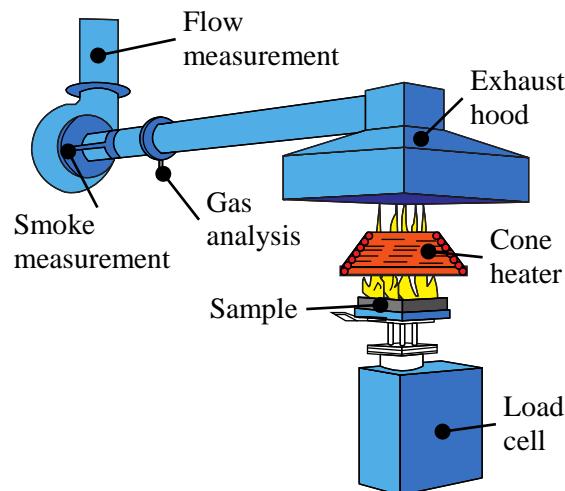


Figure 2. Schematic representation of cone calorimeter

Cone calorimetry is a well-established technique to evaluate flame retardancy of materials. It provides key parameters to assess flame retardant properties of composites. These parameters are the peak of heat release rate (pHRR) [W/m²], the time to ignition (TTI) referring to the delay time [s] between heat exposure and inflammation of the sample, the total heat released (THR) by the combustion [J/m²] and

the effective heat of combustion (EHC), that is the ratio of the THR to the mass loss [J/kg]. Moreover, the percent of char residue at the end of combustion in relation to porosity was considered.

Tests were carried out with the cone calorimeter (Figure 2) from Fire Testing Technology according to the ISO 5660-1 standard. Irradiance was set to 50 kW/m² and each test was made in duplicate in order to assess reproducibility.

3. Results

3.1.1. Microstructure

As expected, Table 3 shows that samples manufactured by injection moulding had almost no porosity. Fused Filament Fabrication (FFF) is expected to induce a non-negligible porosity which was corroborated by these results. Porosity was surprisingly not controlled and varied significantly from one sample to another. In addition, no correlation can be made between samples' porosity and their formulations (constituents and their contents).

Table 3. Mean porosity [%] for each sample depending on its manufacturing process and its thickness of flame-retarded PLA

Processing	PLA	F1	F2	F3	F4	F5	F1'	F2'	F3'	F4'	F5'
INJ	0	0.3	0.7	0.0	0.3	0.5	0.9	0.6	0.1	0.9	0.5
3DP 4 mm	5.7	18.3	7.5	11.2	6.3	7.0	4.7	11	2.8	2.5	2.0
3DP 1 mm	-	9.2	8.1	7.4	8.1	10.2	-	-	-	-	-

The results of these indirect measurements were confirmed by scanning electron micrographs (cf. Figure 3.a). However, microscopy showed also that no gaps were found between filaments of adjacent layers, suggesting good interfaces (cf. Figure 3.b).

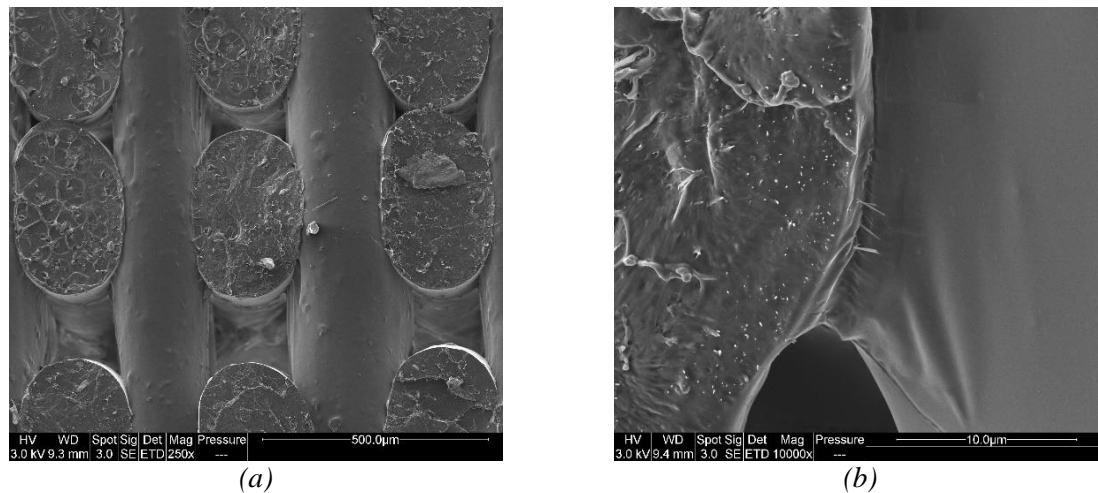


Figure 3. Cross section of a 3DP F4 4 mm plate. (a) 5 layers orthogonal to the horizontal axis, (b) interface between 2 layers

3.1.2. Fire behaviour

Comparing the fire behaviour of INJ and 3DP samples during cone calorimeter tests (cf. Figure 4) shows some differences. Whatever the formulation, little difference can be seen regarding the evolution of HRR according to time, which means that the process does not affect notably the decomposition of samples. However, as shown in Table 4, the THR seems to be slightly lower for 3DP samples. Particularly, the parameter that was the most affected by the process is the TTI (cf. Table 5). The porosity

of 3DP samples seemed to shorten the delay between the moment they started to be radiated and the moment they started to burn. The difference in TTI was up to 22 s in the case of neat PLA.

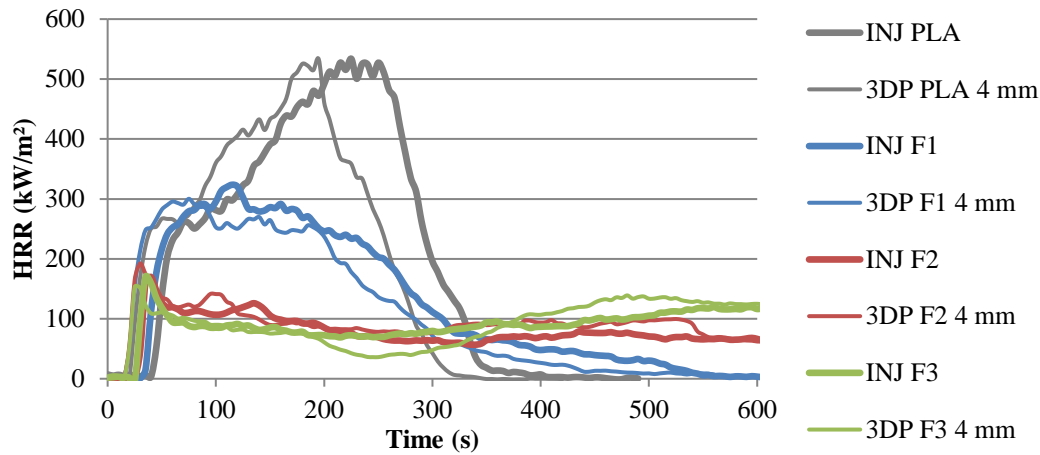


Figure 4. HRR according to radiation time for INJ (thick) and 3DP (thin) samples made of PLA (grey), F1 (blue), F2 (red), and F3 (green)

Table 4. THR [MJ/m²] for each sample depending on its manufacturing process and its thickness of flame-retarded PLA

Processing	PLA	F1	F2	F3	F4	F5	F1'	F2'	F3'	F4'	F5'
INJ	97	79	69	88	98	95	92	94	98	96	96
3DP 4 mm	90	67	68	73	89	86	84	84	93	97	93
3DP 1 mm	-	86	89	87	91	89	-	-	-	-	-

Table 5. TTI [s] for each sample depending on its manufacturing process and its thickness of flame-retarded PLA

Processing	PLA	F1	F2	F3	F4	F5	F1'	F2'	F3'	F4'	F5'
INJ	46	37	28	27	33	33	32	29	27	37	36
3DP 4 mm	24	18	20	19	19	24	23	23	23	26	26
3DP 1 mm	-	23	20	19	23	22	-	-	-	-	-

Table 6. pHRR [kW/m²] for each sample depending on its manufacturing process and its thickness of flame-retarded PLA

Processing	PLA	F1	F2	F3	F4	F5	F1'	F2'	F3'	F4'	F5'
INJ	579	323	178	165	330	514	520	413	505	542	525
3DP 4 mm	532	300	197	156	319	442	512	459	504	515	590
3DP 1 mm	-	481	310	240	486	531	-	-	-	-	-

When adding FR into PLA, as expected, both pHRR and THR decreased, more or less depending on the formulation and the FR content (cf. Table 6 and Table 4). However, the TTI also decreased significantly for all formulations (cf. Table 5).

Comparing the different formulations, the efficiency of F1 turned out to be acceptable for a FR content of 15 wt%. No effect was observed at a FR content of 3.75 wt%. In this case, as shown in Figure 5, the influence of the FR distribution (skin vs whole volume) was not significant.

The efficiency of F2 and F3 with a FR content of 18 wt% was excellent ($\text{pHRR} < 180 \text{ kW/m}^2$). Besides, the influence of the FR distribution was substantial with these formulations. Indeed, at 4.5 wt% of FR, having FR concentrated close to the radiated surface (3DP 1 mm) instead of spread within the whole sample (F'), led to a significant decrease of the pHRR. Regarding pHRR, F3 was more efficient than F2 but a slight difference was observed on TTI and THR.

At 3 wt% of FR, F4 was poorly efficient. No change was observed in TTI and THR compared to PLA, yet there was a significant decrease of the pHRR (approx. 40 %). A lower amount of C30B did not alter the fire behaviour of PLA whatever its distribution in the plate.

Finally, no change was observed in the fire behaviour of PLA with F5 whatever the amount of PS9.

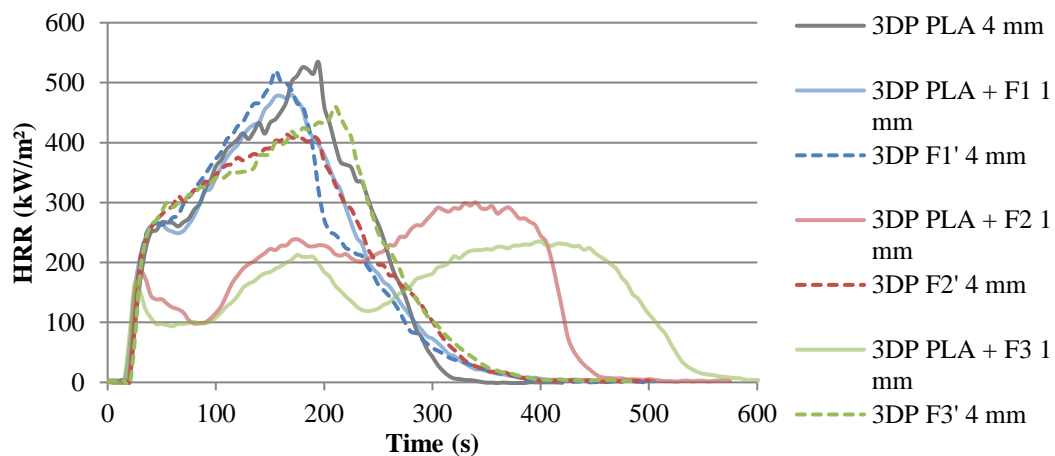


Figure 5. HRR according to radiation time for 3DP samples made of PLA (grey), F1 (blue), F2 (red), and F3 (green), depending on FR distribution (dashed line: in the whole plate – solid line: in the first mm of plate thickness)

4. Discussion

The difference in TTI, and in a lesser extent in THR, between INJ and 3DP samples can be explained by the lower mass of the 3DP samples because of their higher porosity (having a similar apparent volume). In the case of TTI, the temperature increase in the material is expected to be faster for a lighter sample for which heat capacity is lower. Concerning THR, a lower mass induces lesser reactants in the combustion reaction, meaning a lower energy release. This is supported by the EHC values which are globally rather similar (around 17 MJ/kg).

A considerable synergy occurred between APP and MC, on the one hand, and organoclays (both C30B and PS9), on the other [5]. Indeed considered separately, the presence of these constituents in PLA improved poorly its fire behaviour (e.g. F1 and F4) or not at all (e.g. F1', F4', F5, and F5'). When used concomitantly, APP, MC and organoclays helped decreasing drastically the pHRR in the case of F1 (INJ and 3DP 4 mm) thanks to the creation of a protective layer (char) which limited the heating of PLA (cf. Figure 6.a).

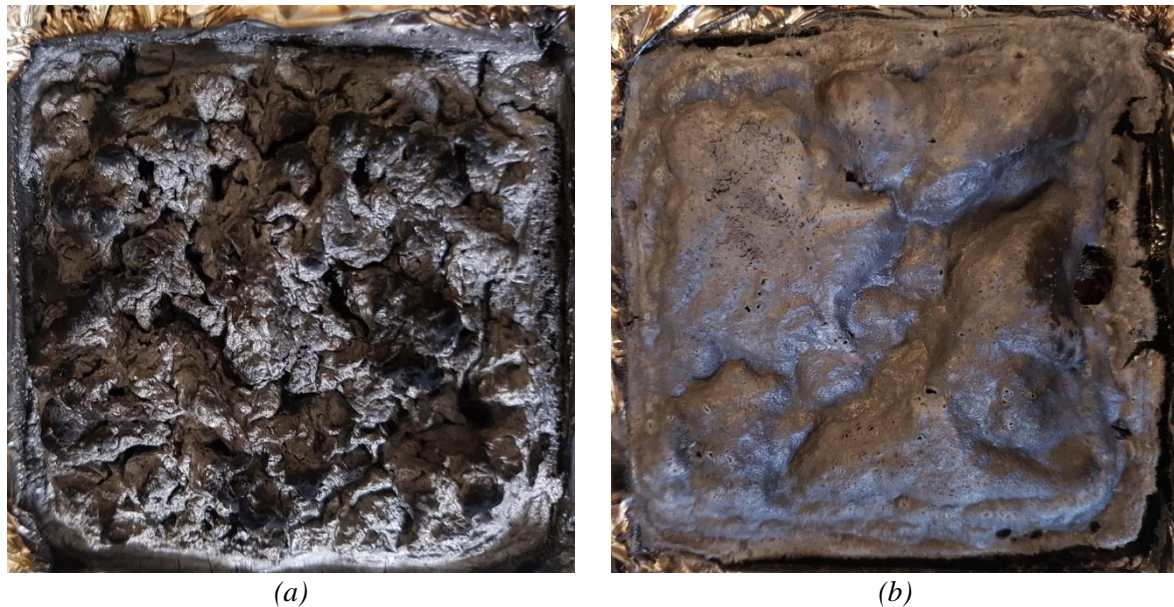


Figure 6. 3DP F1 4 mm (a) and 3DP PLA + F3 1 mm (b) plates after a cone calorimeter test highlighting the presence of a char layer

The results also showed that the distribution of the FR can be decisive in their efficiency. Comparing samples with the same total amount of FR (i.e. 3DP PLA + F 1 mm and 3DP F' 4 mm) showed for F2 and F3 a drastic difference in HRR evolution during cone calorimeter tests. While the behaviour of 3DP F2' 4 mm and 3DP F3' 4 mm did not change much from neat PLA, the pHRR of 3DP PLA + F2 1 mm and 3DP PLA + F3 1 mm decreased by 32 % and 52 % respectively. It is attributed to the difference of formation kinetic of a char layer. In the case of 3DP PLA + F 1 mm, FR were more concentrated close to the surface exposed to radiation, thus forming the char layer from the beginning of the test (cf. Figure 6.b). While in the case of 3DP F' 4 mm, the formation lasted the whole test, making the char less effective.

5. Conclusion

The aim of this study was to identify an appropriate strategy to manufacture 3D printed parts made of flame-retarded PLA by assessing the influence of different compositions made of ammonium polyphosphate, melamine cyanurate and organoclays, the influence of the total amount of FR, and the influence of the FR spatial distribution in PLA.

Results from cone calorimeter tests showed that, compared to injected samples, 3D printed samples sustained a significant decrease in TTI and a slight decrease in THR, both partly caused by the higher porosity (i.e. lower mass) of the latter. Regarding the formulations, the considerable synergy of organoclays with the other FR makes these compositions the most promising in order to decrease the pHRR of flame-retarded PLA.

The most important result of this study would be the benefit of concentrating FR in the vicinity of the radiated surface in order to induce the early formation of a char layer. This turns out to be very advantageous even for complex parts. In slicing softwares used to control 3D printers, flame-retarded PLA could be attributed to shell, bottom, and top layers while the infill structure could be made only of neat PLA, thus with the infill percentage tailoring the mechanical behaviour of the part fabricated in this way. To extend this study, it would be particularly interesting to increase the FR content in the skin part so as to obtain even better fire behaviour.

References

- [1] R.T.L. Ferreira, I.C. Amatte, T.A. Dutra and T. Bürger. Experimental characterization and micrography of 3D printed PLA and PLA reinforced with short carbon fibers. *Composites Part B*, 124: 88-100, 2017.
- [2] L. Dumazert, D. Rasselet, B. Pang and B. Gallard, S. Kennouche. Thermal stability and fire reaction of poly(butylene succinate) nanocomposites using natural clays and FR additives. *Polymers for Advanced Technologies*, (2017) DOI: 10.1002/pat.4090.
- [3] Y. Guo, C.C. Chang, G. Halada, M.A. Cuiffo, Y. Xue, X. Zuo, S. Pack, L. Zhang, S. He, E. Weil and M. H. Rafailovich. Engineering flame retardant biodegradable polymer nanocomposites and their application in 3D printing. *Polymer Degradation and Stability*, 137: 205-215, 2017.
- [4] A. Regazzi, J-M. Lopez Cuesta, L. Dumazert, S. Buonomo and B. Gallard. Efficiency of flame-retarded (FR) PLA compositions for 3D printing. *EuroPolymer Conference EUPOC, Gargnano, Lago di Garda, Italy*, May 21-25 2017.
- [5] S. Hazer, M. Coban and A. Aytac. Effects of the Nanoclay and Intumescent System on the Properties of the Plasticized Polylactic Acid. *ACTA PHYSICA POLONICA A*, 132(3): 634-637, 2017.
- [6] Marius Murariu, Philippe Dubois, PLA composites: From production to properties, *Advanced Drug Delivery Reviews*, 107 (2016) 17-46
- [7] M. Murariu, F. Laoutid, Ph. Dubois, G. Fontaine, S. Bourbigot, E. Devaux, C. Campagne, M. Ferreira, S. SolarSKI, Chapter 21 – Pathways to Biodegradable Flame Retardant Polymer (Nano)Composites, *Polymer Green Flame Retardants*, 2014, Pages 709–773
- [8] Serge Bourbigot and Gaëlle Fontaine, Flame retardancy of polylactide: an overview, *Polymer Chemistry*, (2010) 1413-1422
- [9] Idris Zembouai, Mustapha Kaci, Lynda Zaidi, Stephane Bruzard, Combined effects of Sepiolite and Cloisite 30B on morphology and properties of poly(3-hydroxybutyrate-co-3-hydroxyvalerate)/polylactide blends, *Polymer Degradation and Stability* 153 (2018) 47-52
- [10] Ku Fukushima, Marius Murariu, Giovanni Camino, Philippe Dubois, Effect of expanded graphite/layered-silicate clay on thermal, mechanical and fire retardant properties of poly(lactic acid), *Polymer Degradation and Stability*, Volume 95, Issue 6, June 2010, Pages 1063-1076
- [11] Kuo-Chung Cheng, Cheng-Bin Yu, Wenjeng Guo, Sea-Fue Wang, Tsu-Hwang Chuang, Yan-Huei Lin, Thermal properties and flammability of polylactide nanocomposites with aluminum trihydrate and organoclay, *Carbohydrate Polymers*, Volume 87, Issue 2, 15 January 2012, Pages 1119-1123
- [12] S. SolarSKI, F. Mahjoubi, M. Ferreira, E. Devaux, P. Bachelet, S. Bourbigot, R. Delobel, P. Coszach, M. Murariu, A. Da Silva Ferreira, M. Alexandre, P. Degee, P. Dubois, (Plasticized) Polylactide/clay nanocomposite textile: thermal, mechanical, shrink-age and fire properties, *J. Mater. Sci.* 42 (2007) 5105–5117.
- [13] G. Fontaine, S. Bourbigot, Intumescent polylactide: a non flammable material, *J. Appl. Polym. Sci.* 113 (2009) 3860–3865.